

Jack was delivered by SCHOTT in October 1994. Final inspection revealed outstanding geometrical accuracy and internal quality, in line with the first (and then rated exceptional) achievements made by SCHOTT with Joe. Bubble and inclusion content is extremely low. Compressive stresses around the centre hole are somewhat higher than with Joe, but still within the standard for special quality Zerodur. Transport to REOSC took

quite some time because of bad weather conditions in the Channel. Figure 2 shows Jack's arrival at the REOSC plant at 2:00 a.m. on November 22, 1994. The background shows the new REOSC plant built next to the VLT facility. Since then the axial pads have been glued and grinding is starting. Delivery of the finished mirror (ex works) is scheduled for June 1996.

William should be delivered by SCHOTT in July/August 1995. At the mo-

ment it is under ceramisation and should come out by mid-May for final machining. Averell is under quality inspection prior to grinding its centre hole. Delivery is foreseen in October.

---

For further information please contact:  
P. Dierickx, ESO-Garching,  
e-mail: pdierick@eso.org

# Impact of the Microseismic Activity on the VLT Interferometer

*B. KOEHLER, F. KOCH, ESO-Garching; L. RIVERA, EOPGS, Strasbourg, France*

## 1. Introduction

In a previous article ("Hunting the Bad Vibes at Paranal", *Messenger* No. 76 – June 1994), we described the approach followed by ESO to investigate the effect of microseismic noise on the VLT Interferometer (VLTi). In section 4 of that article, we presented a measurement campaign performed at Paranal to precisely characterise the natural microseismic activity in view of assessing its impact on the VLTi performance. At that date, only preliminary results were available and presented.

This article presents the final results of this campaign which provide the statistical characterisation of the micro-activity as seen from Paranal, as well as the evaluation of its impact on the stability of the Optical Path Length inside the VLT 8-m telescope.

## 2. Characterisation of the Natural Seismic Activity at Paranal

As a preamble to the field experiment at Paranal described in the next sections, the Ecole et Observatoire de Physique du Globe de Strasbourg (EOPGS) performed for ESO a specific processing of the seismic data obtained with its permanent monitoring network installed in the Antofagasta area since 1990. This processing consisted in characterising the seismic activity in that area in terms of earthquakes' magnitude (Richter scale), precise localisation of the sources and frequency of occurrence. Figure 1 illustrates a result of this pre-study. It shows the location of earthquake epicentres and their magnitude for a one-year period (July 1990–June 1991).

### 2.1. Field experiment

The field experiment was carried on from March 21–31, 1994 at Paranal by Dr.

L. Rivera, seismologist from EOPGS, and B. Koehler from ESO-Garching with the logistic support of ESO-Paranal.

Three different kinds of ground motion were recorded during this period: (i) background seismic noise samples in the absence of any seismic events or artificial disturbance, (ii) seismic events due to earthquakes, (iii) human-made noise samples. The noise samples were recorded continuously within pre-defined time windows; with duration ranging from 2 to 10 minutes. The sample frequency used was 500 Hz and occasionally 1000 Hz. Seismic events, on the other hand, were recorded by triggering; the signal was continuously digitised and fed to a detection algorithm which decided whether "an event" was presently arriving. In this case, the recording was activated including a pre-trigger window. A sample frequency of 250 Hz was selected.

All noise samples were recorded during the night at the location of Telescope No. 4. The seismic events were monitored during day and night at the same location but also at the so-called "NTT peak" some 1.5 km north-east from the Paranal top to avoid contamination by human activity during certain days.

The measurement set-up included two types of high-sensitivity seismometers; uni-axial Kinometrics SS-1 and tri-axial Mark-Product L4-3D. Both are velocity transducers based on the spring-mass principle. The inertial motion of the mass/magnet with respect to the outer cage equipped with a coil creates a voltage proportional to the velocity of the seismic mass.

A Reftek 72A-07 seismic station was used to digitise and record the signals coming from the seismometers. The A/D conversion (24 bits) was performed at a very high sample rate of 16 kHz, then a digital FIR filter was used to perform anti-alias filtering of the raw data. Finally the

data were decimated to the selected output sample rate.

A portable Sun Workstation was also brought to the field, in order to read the tapes, visualise the signals and make a preliminary signal analysis.

The resolution and the noise of the whole acquisition chain was carefully computed and experimentally checked. The resolution was  $3 \cdot 10^{-10}$  m/s and the noise power spectral density  $2 \cdot 10^{-10}$  (m/s)/ $\sqrt{\text{Hz}}$ . This very high sensitivity prevented to be limited by the measurement noise even for the very low level of the natural background seismic noise.

### 2.2. Data analysis and results

The total effective time of seismic monitoring by triggering was 125 hours. Figure 2 shows a typical example of recording. A total of 164 events due to earthquakes were recorded during the time mentioned above. For each of them, the following parameters were calculated: (i) the distance of the earthquake epicentre from Paranal, (ii) the seismic moment, (iii) the Richter magnitude and (iv) a parameter representing the level of the local ground acceleration called  $\Gamma$ , and defined later in this section.

Distance between Paranal and the earthquake source were obtained from the so-called, S-P delays. Indeed, even though the propagation speeds of the shear (S) and compression (P) waves varies with the local earth material, their difference is almost a constant. This permits to determine the distance from the difference of arrival times of the two waves. Figure 3 shows a histogram of the number of recorded events as a function of their distance. Some interesting remarks can be made from this histogram (see caption of Figure 3). The most important one is the absence of seismicity closer than 25 km. This indicates the absence of earth-

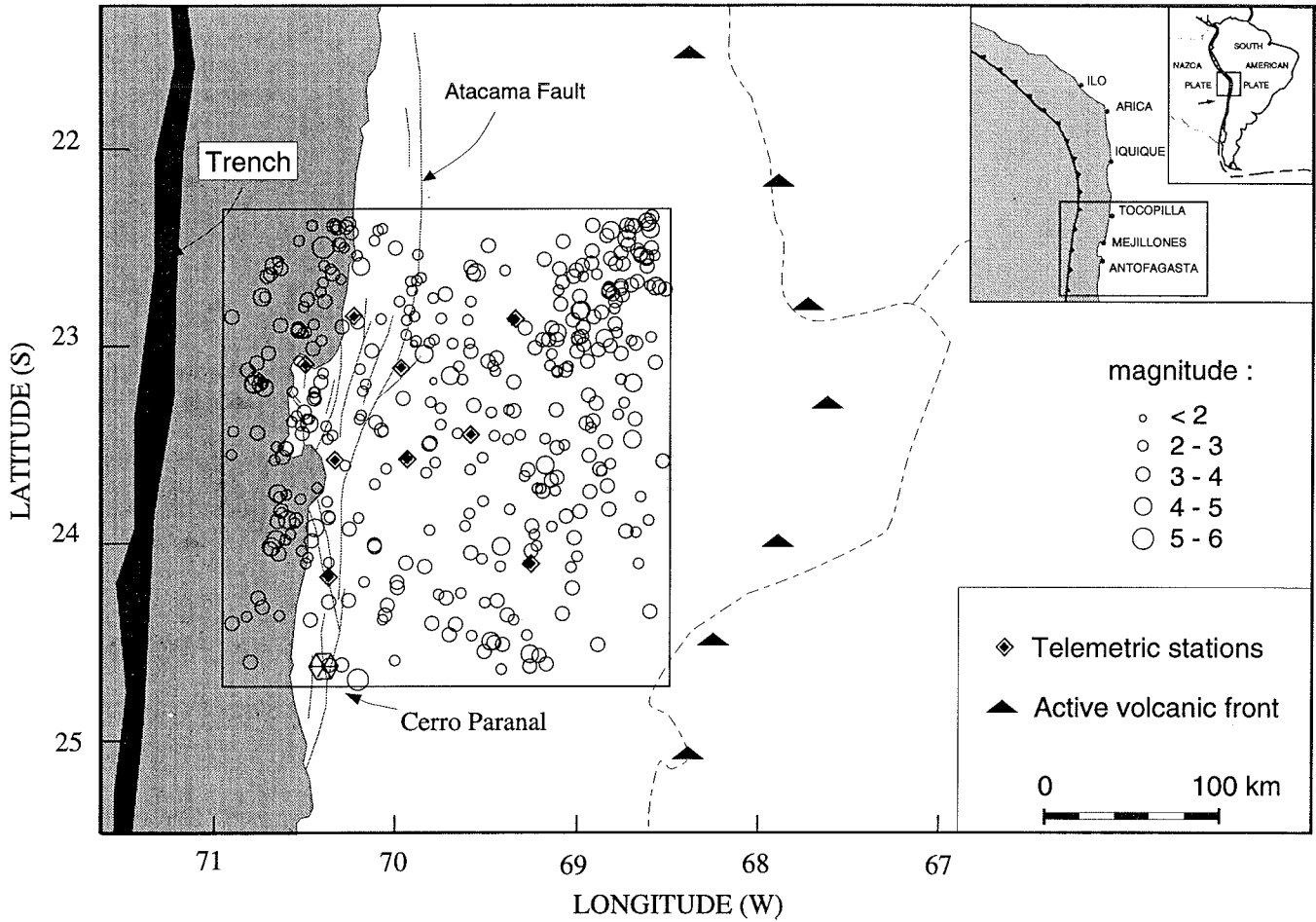
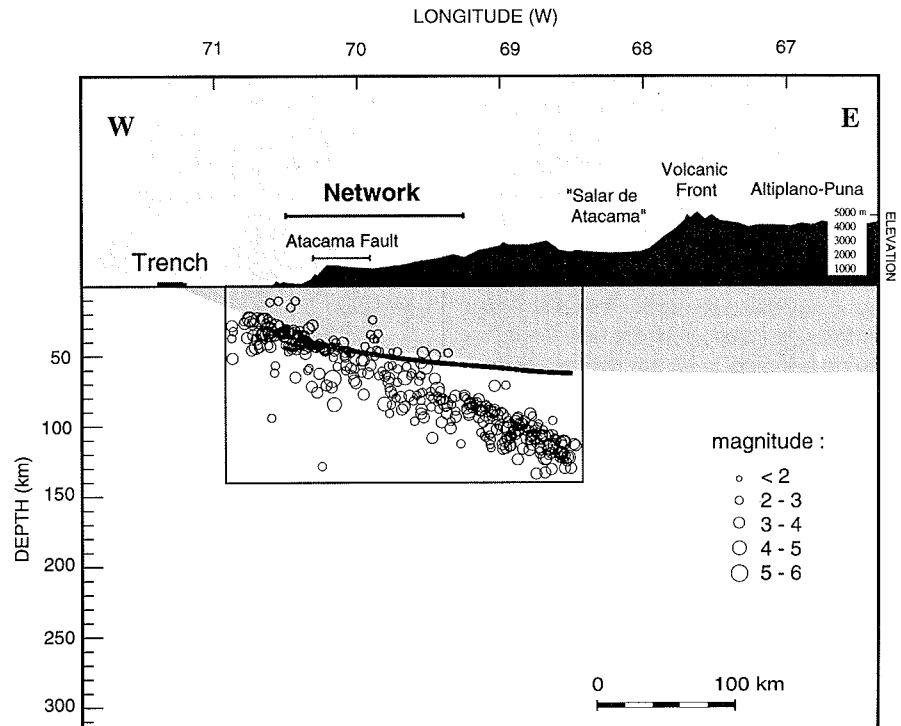


Figure 1: Map and cross-section of the Antofagasta area showing the location of earthquake epicentres and their magnitude for a one-year period (July 1990–June 1991). These maps were generated for ESO by the EOPGS from data collected with its permanent seismic monitoring network.

quake sources very close to the Earth surface which can be particularly destructive (refer, for example, to the effects of such a crustal earthquake in Kobe-Japan in January 1995). This fact is confirmed by the permanent seismic monitoring of the Antofagasta area performed by EOPGS over the last years (see Figure 1). It is also a confirmation of previous observations by the EOPGS that the Atacama Fault, which runs roughly in north-south direction some 4 km east of Paranal, has a very low activity. All that is, of course, very positive for the operation of the VLT since even small events so close from Paranal could produce important acceleration.

A Local Richter Magnitude (ML), which characterises the intrinsic strength of an earthquake, was calculated for each event from the seismogram and taking into account the computed distance. Another measurement of the strength of an earthquake is the Seismic Moment ( $M_0$ ), a well-defined physical value, which is intimately related to the standard dislocation



model for tectonic earthquakes. These parameters which are theoretically linearly related were used to check successfully the homogeneity of the sample. The largest Richter magnitude recorded during the campaign was 5.17 (at 377 km) and the smallest was 0.82 (at 37 km).

The action of an earthquake on the structure of the VLT is, of course, function of the Magnitude (or Seismic Moment) and distance (geometric and intrinsic attenuation). The level of ground acceleration might be the same with a small nearby earthquake or with a larger-distant event.

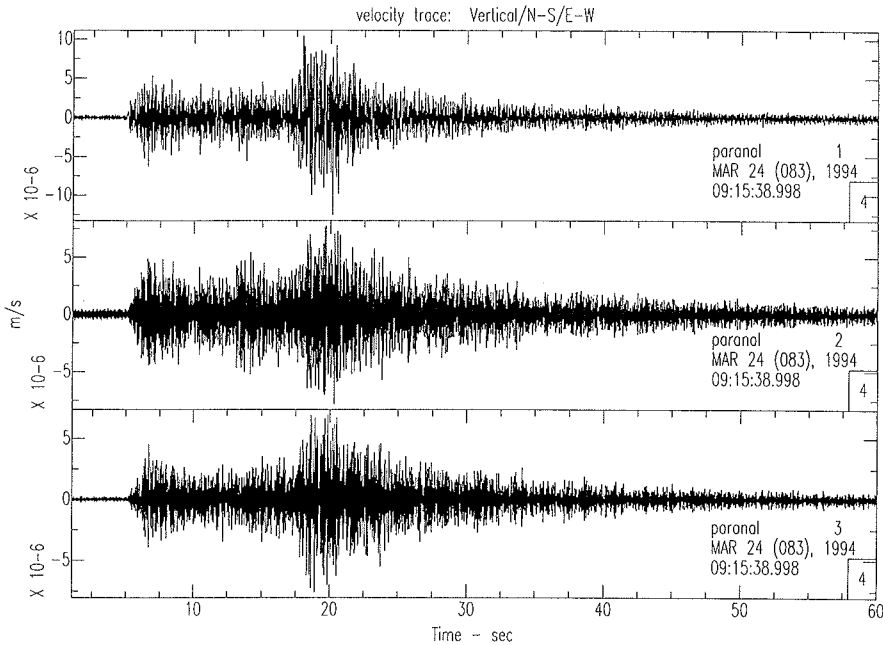


Figure 2: A typical example of recording of a seismic event at Paranal. The start of recording is March 24 at 9 h 15' 39". The three components of the motion (velocity: m/s) are represented against time (sec). From top to bottom: Vertical, N-S and E-W directions. The arrival of the compression wave (P-wave) occurs 5 seconds after the beginning of the record and the shear wave (S-wave) arrives 12 seconds later. This difference of arrival times allows to determine the distance to the earthquake source (here: 100 km). Amplitudes in these three components are quite similar and velocity peaks at about 10  $\mu\text{m/s}$ . Duration of events is of the order of 60–70 seconds.

For this reason, we defined the local parameter  $\Gamma$  as the average level of the ground acceleration Power Spectral Density (PSD) in the frequency range [10–50 Hz] expressed in nano-g/ $\sqrt{\text{Hz}}$ . This parameter is adequate to investigate the effect on the VLTI for two reasons: (i) the acceleration PSD is almost flat (white noise) in this frequency range (in fact up to 100 Hz) and can therefore be characterised by its average, (ii) the most significant structural modes of the VLTI subsystems have frequencies in this range. The smallest  $\Gamma$  value recorded was 6 ng/ $\sqrt{\text{Hz}}$  corresponding to an earthquake of ML = 1.6 at 138 km. The largest value recorded was 9581 ng/ $\sqrt{\text{Hz}}$  corresponding to an earthquake of ML = 4.5 at 160 km. This last event occurred during the night and the acceleration was enough to awake some people at Paranal.

A number of verifications were done to ensure the representativity of the  $\Gamma$  parameter. In particular, the value used later in the analysis, which is computed on the whole 60-second seismogram, was compared with the more instantaneous values obtained on a running window of 2 seconds. It came out that the maximum values of the acceleration PSD reached at the arrival of the P & S wave are very well correlated with the "average" value given by  $\Gamma$  and exceed it by a factor of about 1.5 during some 5 seconds.

The ultimate goal of the campaign was to determine the statistics of the  $\Gamma$  parameter. To this end, a diagram similar to the

so-called Gutenberg-Richter law was constructed. The Gutenberg-Richter law

is used by the seismologists to characterise the seismic activity in a given area. It represents the logarithm of the number of earthquakes with a magnitude higher than M which occurred during a given period versus the magnitude M. The similar diagram for the  $\Gamma$  parameter is shown in Figure 4 for the duration of the experiment (125 hours). As for the standard Gutenberg-Richter law, the relationship is fairly linear. The departure from the linear relationship for low values of  $\Gamma$  (<100 ng/ $\sqrt{\text{Hz}}$ ) is an artefact due to the non-completeness of the sample for these low levels of acceleration which did not always trigger the acquisition.

From Figure 4 we can extrapolate this law for a week (168 hours):

$$\log_{10}(N) = 4.778 - 1.162 \times \log_{10}(\Gamma) \quad (1)$$

Where:

N: number of seismic events during 1 week which exceed the level of acceleration  $\Gamma$

$\Gamma$ : average level of the ground acceleration PSD between 10 and 50 Hz in ng/ $\sqrt{\text{Hz}}$ .

This means that on average each week there is an event with  $\Gamma \geq 13000 \text{ ng}/\sqrt{\text{Hz}}$  or each night one with  $\Gamma \geq 1300 \text{ ng}/\sqrt{\text{Hz}}$  and three events with  $\Gamma \geq 500 \text{ ng}/\sqrt{\text{Hz}}$  or each hour one event with  $\Gamma \geq 160 \text{ ng}/\sqrt{\text{Hz}}$ .

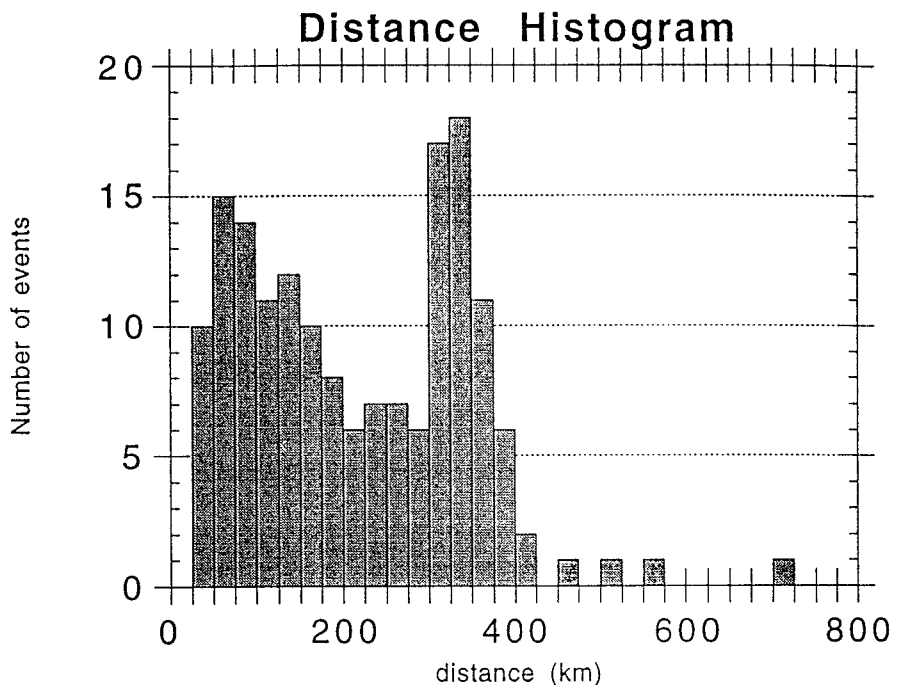


Figure 3: Histogram of the number of earthquakes recorded during the 10-day measurement campaign as a function of their distance from Paranal. The absence of events closer than 25 km comes from the fact that the earthquake sources are located near the subduction plane which lies about 30 km below Paranal (see also Figure 1). Except for the very active zone at 350 km which probably corresponds to a cluster of deep seismic activity already identified by the EOPGS on the Argentinean border, the regular decrease of the histogram is consistent with the simple hypothesis that the earthquakes are uniformly distributed along the subduction plane. Events more distant than 400 km are rare and far enough to be unimportant for the every-day operation of the VLTI.

## Gamma-Frequency law window: 125 hours

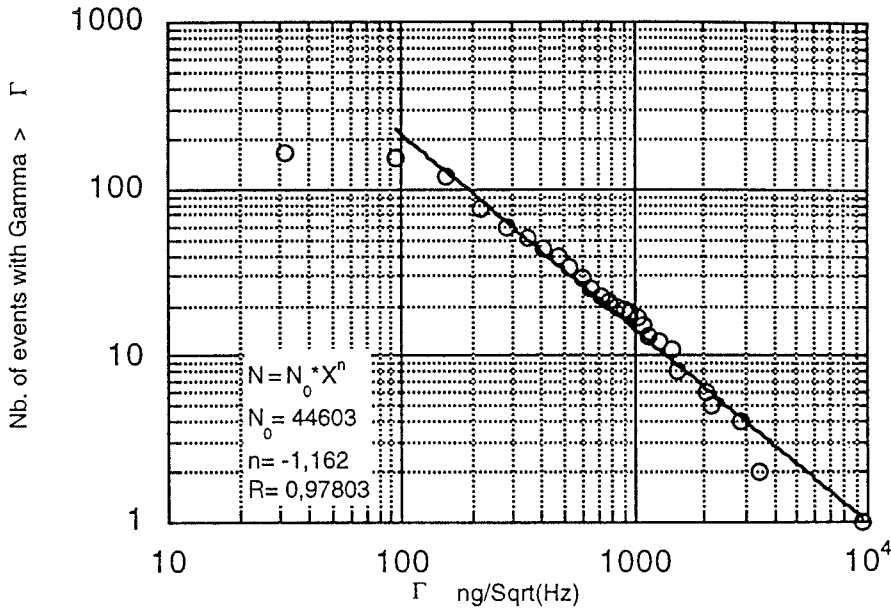


Figure 4: This plot shows the frequency of occurrence of seismic events at Paranal as characterised by the level of ground acceleration they generate. The parameter  $\Gamma$  is the average level of the PSD of the ground acceleration in the frequency range [10-50 Hz]. The Y-axis is the number of events recorded during the 125 hours of the experiment which exceeded the value  $\Gamma$ . Note that the departure from the straight line at  $\Gamma < 100 \text{ ng}/\sqrt{\text{Hz}}$  is due to the non-completeness of the sample.

Figure 5 shows an alternative representation of the same statistics. It represents the probability of exceeding a given acceleration level versus this level for different time windows. It shall be reminded that the sample is not complete for the value of  $\Gamma < 100 \text{ ng}/\sqrt{\text{Hz}}$  and  $\Gamma > 3000 \text{ ng}/\sqrt{\text{Hz}}$  and the curves shall not be used in these ranges.

Because of the short duration of the field experiment in comparison to the recurrence times of large earthquakes in the region, which are of the order of 120 years, it is quite clear that the samples collected in this measurement campaign, or the longer time series obtained by the EOPGS from permanent local networks, north of Cerro Paranal, represent only the seismic activity under relatively "normal" conditions. In order to illustrate the effect of a large earthquake on the seismic regime, the Alaskan earthquake (Magnitude 9.2) which occurred on March 28, 1964 was used. This well-documented event, though larger than what could be expected in northern Chile, is tectonically similar and also located in a subduction zone. The long-term seismic monitoring shows that the level of background seismicity can increase by a factor larger than 10 during the first year after the main earthquake and that more than one year may be required to return to a level of seismicity comparable to what existed before the earthquake.

### 3. Impact of the Natural Seismic Activity on the VLTI

#### 3.1. Description of the method to assess the OPD variation inside the VLTI 8-m telescope

With the detailed characterisation of the seismic activity described above, the

impact on the VLT (and more particularly the VLTI) can be assessed. We present in the following the computations and the results obtained for the VLTI 8-m telescope.

Similar computations are necessary on the VLTI Auxiliary Telescope and on the Delay Line. Less detailed computations were performed for these subsystems during their feasibility studies. The assessment of micro-seismic effects will have to be updated according to their final design, but we anticipate these effects to be less important than on the 8-m telescope, for various reasons.

The goal of the computation is to evaluate the time variation of the Optical Path Length inside the telescope from M1 to the Coudé focus due to mirror vibration. This will be referred to as Optical Path Differences (OPD) in the following.

For that purpose, a detailed Finite Element Model of the telescope was built by F. Koch using substructure models developed by the contractors of the various telescope parts. The model consists of the telescope pier, a complete structural model of the telescope structure including hydraulic bearings and all mirrors and their supports down to the Coudé focus. The model contains 24,000 elements and 95,000 degrees of freedom. It is shown in Figure 6.

The computation consists of the following steps: (i) computation of the transfer functions (or harmonic responses) between an input ground motion in X, Y or Z directions and the displacements of each individual mirror, (ii) computation of the global OPD transfer function corresponding to the above motions using an optical sensitivity matrix, (iii) computation of the PSD of OPD variation by multiplica-

### Exceeding Probability (window: 125 hours)

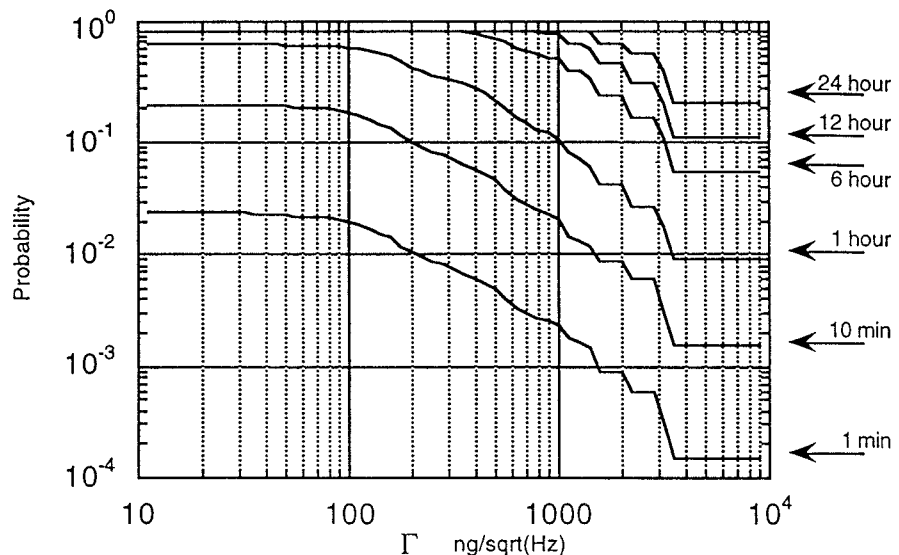


Figure 5: This plot shows the probability of occurrence of seismic events exceeding a given  $\Gamma$  value during different time windows.

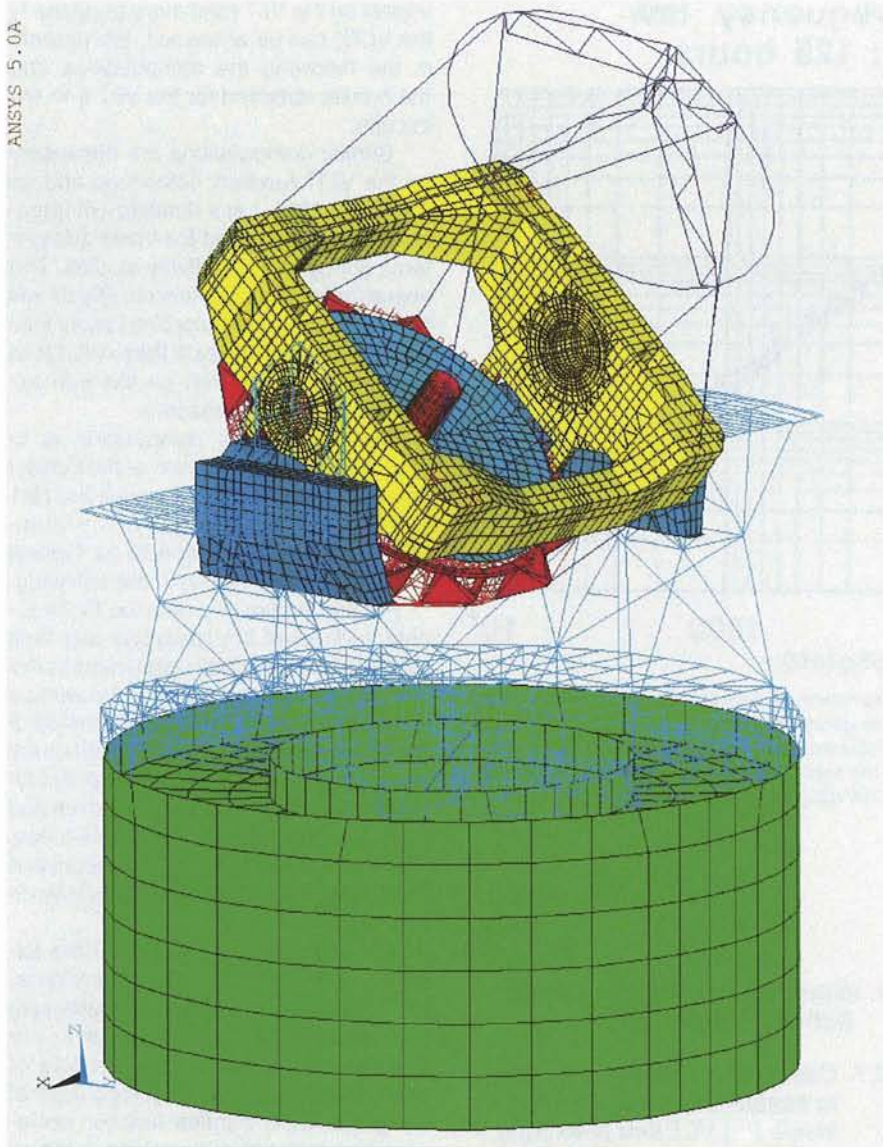


Figure 6: Finite Element Model of the VLT 8-m telescope used to assess the impact of seismic activity on the VLTI performance. The model consists of the telescope pier, a complete structural model of the telescope structure including hydraulic bearings and all mirrors and their supports down to the Coudé focus. The model contains 24,000 elements and 95,000 degrees of freedom.

tion of the PSD of the ground motion with the square of the global OPD transfer function, (iv) computation of the OPD variation on a given exposure time by integration of the properly weighted PSD of the OPD.

### 3.2. Results

Figure 7 shows the OPD transfer functions obtained for each direction of ground motion. The amplification due to the numerous structural modes is clearly visible. The major amplification factors occur in the Z direction (vertical) in the 50 to 70 Hz region. They correspond to the local modes of the supports of the Coudé mirrors M5, M6 and M8.

Figure 8 illustrates, as an example, the effect of the seismic event recorded on

March 26 at 03:36 UT. This event has a  $\Gamma$  of  $510 \text{ ng}/\sqrt{\text{Hz}}$  (i.e. a type of event

TABLE 1.

Exposure time (msec)	10	48	290
Observing wavelength ( $\mu\text{m}$ )	0.6	2.2	10
Specifications (nm RMS)	14	50	225
OPD variation under natural background seismic noise (nm RMS)	3	12	72
OPD variation for a seismic event of $\Gamma = 510 \text{ ng}/\sqrt{\text{Hz}}$ (nm RMS)	64	109	119

TABLE 2.

Observing wavelength ( $\mu\text{m}$ )	0.6	2.2	10
Disturbing threshold $\Gamma_0$ ( $\text{ng}/\sqrt{\text{Hz}}$ )	110	234	964
Period of recurrence of disturbing events	40 min.	1 h 40 min.	8 h

occurring typically 3 times per night). The resulting OPD variation together with the VLTI specifications is given in Table 1. The specifications are derived from the error budget of the fringe contrast decrease corresponding to different observing wavelengths. The OPD variation under the natural background seismic noise (i.e. in the absence of any seismic events or artificial sources) is also given for comparison.

This shows that the VLTI performance will be degraded (with regard to the present error budget) for events with magnitude and frequencies of occurrence as given in Table 2.

In case of occurrence of an event larger than the above thresholds, the performance of the interferometer will be degraded for about 1 minute (see Fig. 2).

Figure 5 can also be used to assess the probability of exceeding the above values for given observing windows. For example during an observation of 10 minutes, the probability to exceed the disturbing threshold in the visible, near-IR and IR is respectively  $\approx 20\%$ ,  $8\%$  and  $2\%$ .

In parallel to the assessment of OPD variations presented above, the impact of seismic events on the image motion at the Coudé focus was evaluated and was found to be negligible; an event of  $\Gamma = 510 \text{ ng}/\sqrt{\text{Hz}}$  creates 5 milli-arcseconds RMS of pointing error.

## 4. Conclusion

The results presented above evidence an important impact of the seismic activity at Paranal on the VLTI performance. The bottom line is that the fringe contrast will be significantly affected, for periods of about 1 minute, by seismic events occurring, on the average, every 40 minutes for observations in the visible and every 1 hour 40 minutes for near-IR observations. Such an impact is not dramatic, but cannot simply be ignored.

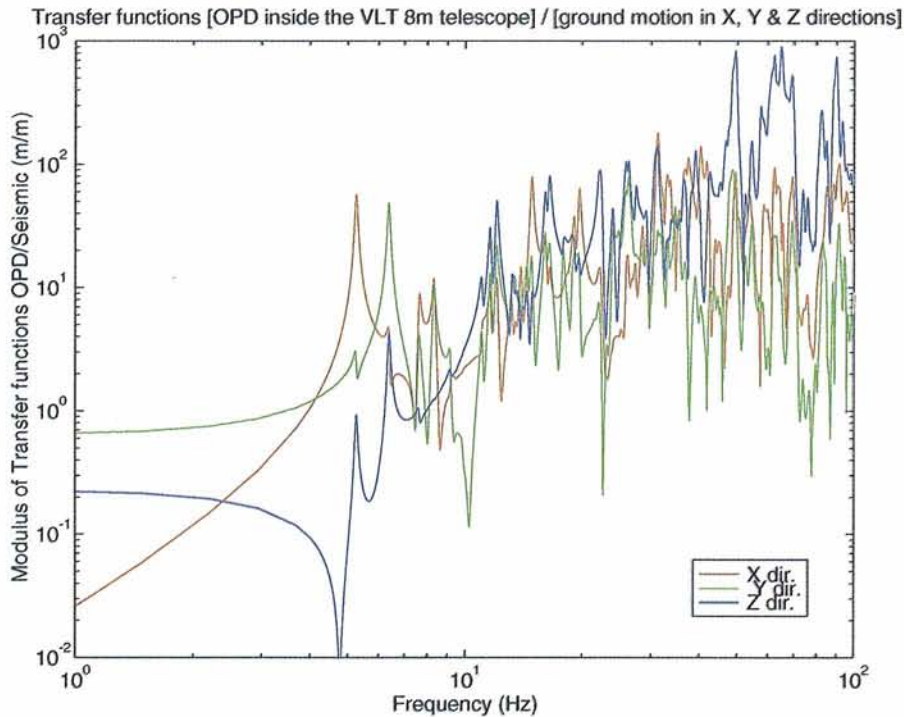


Figure 7: Transfer functions relating the OPD variation inside the VLT 8-m telescope to an input ground motion. The curves represent the ratio of the OPD over the input ground displacements in X (along altitude axis), Y (horizontal, perpendicular to the altitude axis), and Z (vertical) directions versus the frequency of the displacement. The peaks and valleys are all related to structural modes. The highest amplification factors, driving the final OPD stability, occur at 50 Hz and between 60–70 Hz in the Z direction. They are related to modes of the supports of the Coudé mirrors M5, M6 and M8.

The immediate consequence is the need to monitor the seismic activity at the site during VLTI operation with the 8-m telescopes. For this purpose, a seismic monitoring system will be included in the Astronomical Site Monitor of the VLT. It will consist of several seismometers monitoring the ground acceleration on the site. They will inform the VLTI Control System of the occurrence of any significant seismic events to allow immediate action to be taken (e.g., close the instrument shutter in case of long exposures) and will store in a data base the recorded ground accelerations to be used during post-processing (e.g., for identification of corrupted snapshot exposures).

A second consequence can be drawn from the detailed analysis of the OPD spectrum resulting from seismic events. The major part of the OPD variation energy over short exposures originates from the excitation of local axial modes of the support of mirrors M5, M6 and M8 in the Coudé train of the 8-m telescope and not from global modes of the telescope structure. This means that optimisation of these supports by increased stiffness or damping shall be considered during their final design and that improvement of the results presented in this article may be expected.

The third consequence concerns a metrology system based on laser interferometer and accelerometers which

could be developed to monitor in real time the OPD variations inside the telescope in view of their correction with the PZT-

mounted secondary mirror of the VLTI Delay Lines. In fact, such a system has been considered since the early stage of the VLTI project, and provision has been included in the design of the telescope to allow, if necessary, its future implementation such as a space for a retro-reflecting device at the centre of the secondary mirror. Even though the studies of other disturbances such as wind load, artificial vibration sources, etc. have shown that such a metrology is not essential, the present results indicate that it is prudent to study its feasibility and its design in order to allow its quick implementation if it appears necessary and feasible.

As a last consequence, we can wonder if the early knowledge of the results of such a detailed analysis would have impaired the selection of Paranal as the VLT/VLTI site. Indeed, the loss in observing time due to microseismic activity (1 min./40 min. = 2.5 % in the worst case) remains negligible with regard to the gain (up to 200 %) due to improved seeing and cloud conditions (see VLT Report No. 62).

For further information please contact:  
B. Koehler, ESO-Garching.  
E-mail: bkoehler@eso.org, Tel:  
+40 (89) 320 06 515, Fax: +49 (89) 320 23 62.

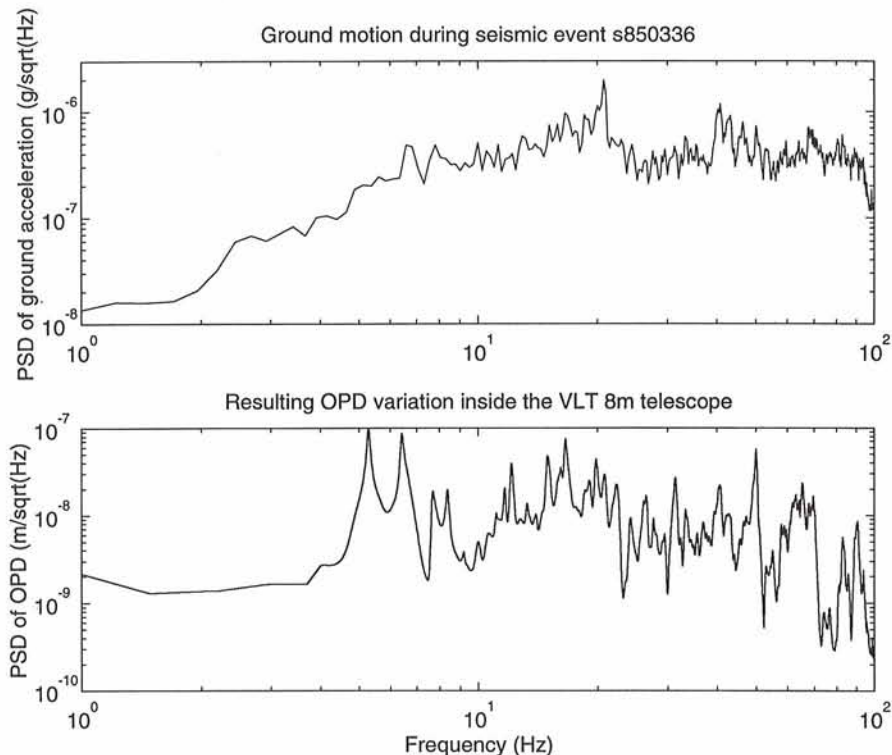


Figure 8: Effect of a seismic event on the OPD variation inside the VLT 8-m telescope. The event was recorded on March 26 at 03:36 UT. It is a type of event occurring typically 3 times per night. Upper: Power Spectral Density (PSD) of the ground acceleration measured at Paranal. Lower: PSD of the resulting OPD inside the telescope.